

12-6-2023

## Lining–stratum interaction mechanism of mountain tunnel based on static pushover model test

Qin-wu LU

*College of Civil Engineering, Fuzhou University, Fuzhou, Fujian 350116, China, lqw5467@163.com*

Zhen-chang GUAN

*College of Civil Engineering, Fuzhou University, Fuzhou, Fujian 350116, China, gaussto@hotmail.com*

Lin LIN

*College of Civil Engineering, Fuzhou University, Fuzhou, Fujian 350116, China*

Shu-jing WU

*College of Civil Engineering, Fuzhou University, Fuzhou, Fujian 350116, China*

*See next page for additional authors*

Follow this and additional works at: <https://rocksoilmech.researchcommons.org/journal>



Part of the [Geotechnical Engineering Commons](#)

---

### Recommended Citation

LU, Qin-wu; GUAN, Zhen-chang; LIN, Lin; WU, Shu-jing; and SONG, De-jie (2023) "Lining–stratum interaction mechanism of mountain tunnel based on static pushover model test," *Rock and Soil Mechanics*: Vol. 44: Iss. 8, Article 4.

DOI: 10.16285/j.rsm.2022.6300

Available at: <https://rocksoilmech.researchcommons.org/journal/vol44/iss8/4>

This Article is brought to you for free and open access by Rock and Soil Mechanics. It has been accepted for inclusion in Rock and Soil Mechanics by an authorized editor of Rock and Soil Mechanics.

---

## Lining–stratum interaction mechanism of mountain tunnel based on static pushover model test

### Abstract

With the rapid development of traffic infrastructure construction in western mountain area, the lining-stratum interaction mechanism of mountain tunnel under seismic effects has attracted increasing attentions. Based on the prototype of a regular two-lane highway tunnel section with V-grade surrounding rock, a static pushover model test for mountain tunnel was conducted. The variations of stratum displacement, stratum strain and ground pressure with pushover distance were carefully studied, and the lining-stratum interaction mechanism was thoroughly discussed. The test results show that: the lining-stratum interaction can be generally divided into compacting stage, overturning stage, and dragging stage. The stratum tends to circumferentially flow along the lining perimeter from the springing line in the overturning stage, and then drives the lining to shift together in the dragging stage. The stratum near the springing line experiences predominantly radial compression, forming a compression deformation zone, while the stratum near the lining shoulder mainly undergoes circumferential compression, forming a slip deformation zone. The response of the ground pressure on the left and right sides are exactly opposite. Specifically, the ground pressure in the compression deformation zone on the right side is greater than its counterpart on the left side, while the ground pressure in the slip deformation zone on the right side is less than its counterpart on the left side. These researches can provide some experimental basis and technical support for the anti-seismic calculation of mountain tunnels based on response displacement method.

### Keywords

mountain tunnel, lining–stratum interaction mechanism, static pushover model test, digital image correlation, ground pressure

### Authors

Qin-wu LU, Zhen-chang GUAN, Lin LIN, Shu-jing WU, and De-jie SONG

# Lining–stratum interaction mechanism of mountain tunnel based on static pushover model test

LU Qin-wu, GUAN Zhen-chang, LIN Lin, WU Shu-jing, SONG De-jie

College of Civil Engineering, Fuzhou University, Fuzhou, Fujian 350116, China

**Abstract:** With the rapid development of traffic infrastructure construction in western mountain area, the lining–stratum interaction mechanism of mountain tunnel under seismic effects has attracted increasing attentions. Based on the prototype of a regular two-lane highway tunnel section with V-grade surrounding rock, a static pushover model test for mountain tunnel was conducted. The variations of stratum displacement, stratum strain and ground pressure with pushover distance were carefully studied, and the lining–stratum interaction mechanism was thoroughly discussed. The test results show that: the lining–stratum interaction can be generally divided into compacting stage, overturning stage, and dragging stage. The stratum tends to circumferentially flow along the lining perimeter from the springing line in the overturning stage, and then drives the lining to shift together in the dragging stage. The stratum near the springing line experiences predominantly radial compression, forming a compression deformation zone, while the stratum near the lining shoulder mainly undergoes circumferential compression, forming a slip deformation zone. The response of the ground pressure on the left and right sides are exactly opposite. Specifically, the ground pressure in the compression deformation zone on the right side is greater than its counterpart on the left side, while the ground pressure in the slip deformation zone on the right side is less than its counterpart on the left side. These researches can provide some experimental basis and technical support for the anti-seismic calculation of mountain tunnels based on response displacement method.

**Keywords:** mountain tunnel; lining–stratum interaction mechanism; static pushover model test; digital image correlation; ground pressure

## 1 Introduction

China is situated between the Pacific Seismic Belt and the Eurasian Seismic Belt. Particularly in the hilly and mountainous regions of the west, there are significant variations in terrain and numerous active faults, and the earthquake intensity resistance are generally above VIII<sup>[1]</sup>. As China's transportation construction advances towards the western regions, the interaction mechanism between mountain tunnel lining and strata under seismic action has become a challenge and hot topic of research in both academic and industrial communities<sup>[2–3]</sup>.

Various model tests, including shaking table tests, centrifuge tests, and quasi-static pushover tests, are effective means to investigate the interaction mechanism between mountain tunnel lining and strata. Compared to costly dynamic tests, quasi-static pushover tests are not only cost-effective but also more closely resemble the response displacement method commonly used in anti-seismic calculations, hence they are widely adopted in both academia and industry. Jing et al.<sup>[4]</sup> conducted a large-scale pushover test on single-layer box-type underground structures in the sandy ground to study the evolution of soil horizontal subgrade coefficient with loading level. Xu et al.<sup>[5]</sup> carried out a series of pushover tests on the Dakai station to quantitatively investigate the structure–stratum interaction mechanism.

Chen et al.<sup>[6]</sup> conducted a large-scale pushover test on a multi-layer subway station, focusing on the crack propagation process and failure mode of the station structure. Xu et al.<sup>[7]</sup> proposed a spring-underground structure system for quasi-static pushover tests considering soil–structure interaction and conducted in-depth research on the weak positions and failure mode of the Dakai station model. Liu et al.<sup>[8]</sup> and Han et al.<sup>[9]</sup> mainly examined the influence of model container types and lateral boundary displacement distributions on the results of static pushover tests.

To summarize, significant progress has been made regarding the structure–stratum interaction mechanism of rectangular section structures under quasi-static pushover effects. However, the unique horseshoe-shaped section and complex and variable surrounding rock conditions of mountain tunnels make their seismic response significantly different from rectangular structures<sup>[10–11]</sup>. This paper presents the results of a quasi-static pushover model test on the conventional cross-sectional mountain tunnel, and explores the changes in stratum displacement, stratum strain, and ground pressure with pushover displacement. It further unveils the lining–stratum interaction mechanism under seismic effect in mountain tunnels, providing experimental basis and technical support for the anti-seismic calculation of mountain tunnels based on the response displacement method.

Received: 22 August 2022

Accepted: 13 December 2022

This work was supported by the National Natural Science Foundation of China (52278399) and the Natural Science Foundation of Fujian Province (2021J01599).

First author: LU Qin-wu, male, born in 1995, PhD candidate, mainly engaged in the research on tunnel engineering. E-mail: lqw5467@163.com

Corresponding author: GUAN Zhen-chang, male, born in 1980, PhD, Professor, PhD supervisor, mainly engaged in the research and teaching works on geotechnical and tunnel engineering. E-mail: gaussto@hotmail.com

## 2 Response displacement method and quasi-static pushover test mechanism

### 2.1 Classical response displacement method

The classical response displacement method, as a recommended method for the aseismic design of underground structures, has been widely promoted and applied<sup>[12–13]</sup>. The anti-seismic calculation of a cross-section is presented as an example, its primary loads include the relative displacement of the stratum, the inertial force of the structure, and the shear force from the surrounding stratum. Foundation springs are introduced to simulate the interaction between the stratum and the structure, as shown in Fig. 1.

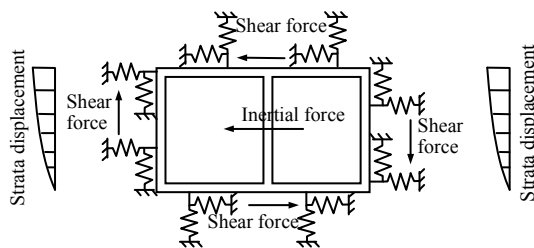


Fig. 1 Diagram of classic response displacement method

The classical response displacement method has a clear mechanical mechanism and offers relatively simple calculations. However, it is difficult to directly account for the structure–stratum interaction (such as the difficulty in determining the stiffness of the foundation springs, and the presence of complex contact forces on irregular underground structures). Therefore, many scholars have successively proposed improved calculation methods, such as the integral response displacement method<sup>[14]</sup> and the boundary forced response displacement method<sup>[15]</sup>.

### 2.2 Boundary forced response displacement method

The boundary forced response displacement method proposed by Du Xiuli's team<sup>[15]</sup> applies seismic loads on the model boundary in the form of forced displacements. This allows for a direct consideration of the structure–stratum interaction, as illustrated in Fig.2. Initially, the boundary displacement  $U_1$  corresponding to the designed peak surface displacement  $U_0$  is determined from a free-field pushover test. By applying this displacement to the lateral boundary of the structure–stratum system, the mechanical response of the structure under seismic action can be directly and accurately calculated.

The static pushover model test for underground structures serves as the experimental foundation for the aforementioned boundary forced response displacement method<sup>[4–7]</sup>. Many scholars have explored the structure–stratum interaction mechanism under seismic conditions through pushover tests of rectangular or circular underground structures with an inverted triangular displacement imposed on their boundaries. Unlike regular cross-sectional shapes like rectangles or circles, this paper takes the horseshoe-shaped mountain tunnel as the research object to explore the changes in stratum displacement, stratum strain, and

ground pressure with pushover displacement.

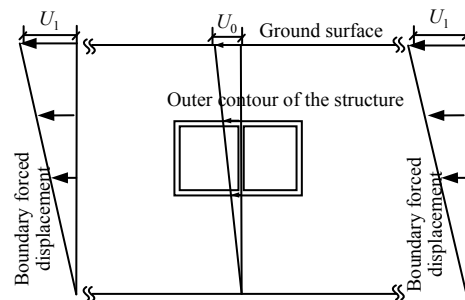


Fig. 2 Diagram of boundary forced response displacement method

## 3 Static pushover model test

### 3.1 Similarity ratio design and selection of similar materials

For a standard two-lane highway tunnel with surrounding rock of Grade V as a prototype, the inner contour consists of an arch ring, sidewall, and invert arch. The radii of the arch ring and invert arch are 4.85 m and 15 m, respectively. The secondary lining is constructed using C30 reinforced concrete with a thickness of 0.4 m; the maximum span and height of the outer excavation contour are 10.5 m and 8.4 m, respectively.

Based on the principle of dimensional similarity, a scale-down model was designed. Firstly, considering the test site conditions, a length similarity ratio of  $S_L = 1/40$  was selected. Then, based on the experience in preparing similar materials for strata, an elastic modulus similarity ratio of  $S_E = 1/40$  was chosen. As the acceleration similarity ratio  $S_g$  was constantly 1, other physical quantities could be determined according to the principle of dimensional similarity, as shown in Table 1.

Table 1 Design of similarity ratio in model test

Type	Parameter	Relationship formula	Similarity ratio
Material property	Cohesion $c$	$S_c = S_E$	1/40
	Internal friction angle $\varphi$	$S_\varphi$	1
	Elastic modulus $E$	$S_E$	1/40
	Poisson's ratio $\mu$	$S_\mu$	1
Geometric feature	Density $\rho$	$S_\rho = S_E / (S_g S_L)$	1
	Length $L$	$S_L$	1/40
	Area $S$	$S_S = S_L^2$	1/1 600

Shallowly buried strata are usually mainly composed of V-grade surrounding rock. Referring to previous research<sup>[16]</sup>, using quartz sand as the aggregate, and bentonite and gypsum as auxiliary materials, the stratum similar material was obtained with a mass ratio of quartz sand: bentonite: gypsum: water = 0.747: 0.108: 0.026: 0.119. The measured density is 1.83 g/cm<sup>3</sup>, cohesion is 0.46 kPa, and the internal friction angle is 32.0°, which basically meets the physical and mechanical parameter requirements of V-grade surrounding rock (after conversion through similarity

ratio).

The lining model was cast with gypsum, with a water-to-gypsum ratio  $w/p$  selected as 1.3:1. Its elastic modulus was estimated to be 2.3 GPa using the following formula, with a Poisson's ratio of 0.25<sup>[17]</sup>.

$$E_m = 3.6(p/w - 0.1w/p) \quad (1)$$

Further, based on the bending stiffness similarity principle as shown in the following equation, the thickness of the lining model  $h_m$  was calculated to be 23.5 mm.

$$h_m = \frac{h_p}{S_L} \left[ \frac{E_p(1-\mu_m^2)}{E_m(1-\mu_p^2)} \right]^{1/3} \quad (2)$$

where the elastic modulus of the lining prototype is  $E_p = 30$  GPa, the Poisson's ratio is 0.25, and the thickness is 0.4 m. Based on the above, the geometric dimensions of the lining model for the standard two-lane road tunnel are shown in Fig. 3.

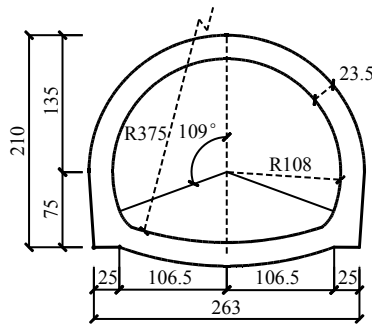


Fig. 3 Lining model of two-lane highway tunnel (unit: mm)

### 3.2 Model container design

Considering the boundary effect, the overall dimensions of the static pushover model container are designed to be 2.4 m×1.4 m×0.6 m (width×height×thickness), as shown in Fig. 4. The front, back, left, and right walls are all composed of transparent acrylic plates bolted to a square steel frame: The front and back walls are bolted and fixed to the bottom plate, while the left and right walls are hinged to the front and back walls via a rotating shaft at the bottom, allowing them to rotate about the wall toe. At the top of the model container, there are push–pull rods and plane-holding rods, ensuring that the left and right walls always move synchronously during the pushover

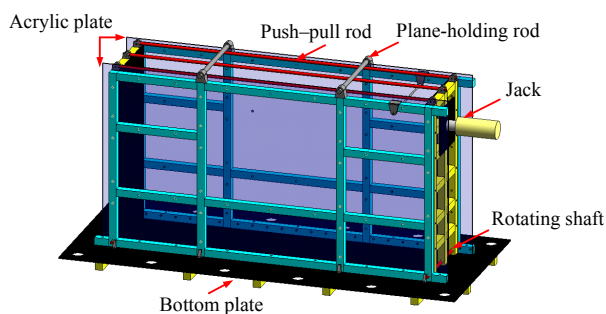


Fig. 4 Illustration of model container in static pushover test

process, and the front and back walls always remain in a plane strain state.

The bottom plate is bolted to the ground using anchor bolts (not shown in the figure); a small jack is used to apply an inverted triangular pushover displacement to the right wall, and its reaction force is borne by a reaction wall (also not shown in the figure).

### 3.3 Loading conditions and measurement system

Relevant codes<sup>[12–13]</sup> stipulate that under E3 seismic actions, the designed peak surface displacement for a Class IV site (corresponding to a peak acceleration of 0.4g) is 0.7 m. Based on the geometric similarity ratio, the peak surface displacement in the model test (denoted as  $U_0$ ) is calculated to be 17.4 mm. Preliminary static pushover tests were first conducted in open fields to obtain the boundary pushover displacement corresponding to the peak surface displacement  $U_1$ , which is approximately 100 mm.

In the static pushover test for the mountain tunnel, an inverted triangular pushover displacement with a 5 mm increment was gradually applied to both right and left boundaries until the maximum pushover displacement reached 100 mm, as shown in Fig. 5. The total height of the stratum model is 1.2 m, and the burial depth of the lining model is 0.29 m (shallow burial situation).

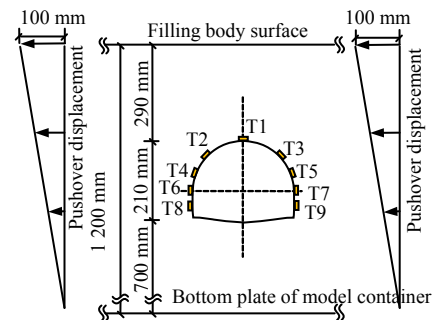


Fig. 5 Overall schematic diagram of static pushover test (unit: mm)

Based on the digital image correlation technology (detailed in Section 4.1), the displacement and strain responses of the stratum were calculated by precisely measuring the changes in speckle coordinates in continuous photographs. Nine mini soil pressure boxes were closely affixed to the external surface of the lining model to monitor changes in the ground pressure, as shown in Fig. 5. Specifically, T1 was located at the arch crown of the lining, while T3, T5, T7, and T9 were respectively positioned at the right shoulder, hance, springing line, and sidewall of the lining. T2, T4, T6, and T8 were symmetrically arranged on the left side of the lining.

### 3.4 Testing process

Lining model production. Customized lining molds were designed according to the similarity ratio. The gypsum slurry was mixed according to the designed water–plaster ratio and poured into the mold. After solidification and molding, the mold was removed to form the lining model, as shown in Figs. 6(a) and 6(b).

Stratum similar material preparation and filling. Quartz sand, bentonite, gypsum, and water were mixed evenly according to the designed ratio and were layered. Each layer was then compacted according to density requirements. The lining model with tightly adhered miniature earth pressure boxes was placed at a height of 0.7 m, as shown in Fig. 6(c). The filling continued until it reached a height of 1.2 m.

Loading process. Two fixed cameras were positioned to focus on the observation area, and a bright light source and surrounding shading cloth were set up, as shown in Fig.6(d). The jack was then activated to gradually apply an inverted triangle pushover displacement to the right wall at an interval of 5 mm until the maximum pushover displacement of 100 mm was reached.



Fig. 6 Implementation of static pushover test

## 4 Stratum displacement analysis

### 4.1 Introduction to digital image-related techniques

Digital image correlation (DIC) technology is based on the principle of speckle image correlation analysis. High-precision measurement of the surface coordinates of the object during deformation is achieved by tracking the speckle images on the surface of an object. DIC technology can capture the overall displacement and strain within the image range of the stratum, providing possibilities for studying the interaction between structures and strata.

The DIC-integrated programs PhotoInfor and Postview used in the model test were developed by China University of Mining and Technology. The former was used for image analysis, and the latter was for post-processing<sup>[18]</sup>. The specific procedure is as follows: Continuously captured images during the static pushover process are imported into PhotoInfor. The scale is set as 0.149 mm/pixel based on the ratio of image pixel to actual size. An auxiliary grid is

established and imported into PhotoInfor, as shown in Fig.7. The data files obtained from PhotoInfor are imported into Postview for further processing, resulting in cloud diagrams of stratum displacement and strain in key focus areas.

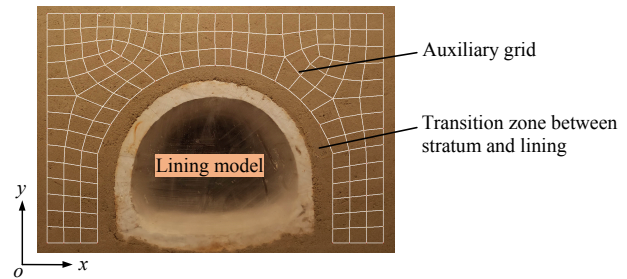


Fig. 7 Critical focus area and auxiliary grid

It should be noted that the auxiliary grid did not closely adhere to the lining model but instead left a transition zone of 20 mm between them. Due to the significant squeezing effect between the lining and the stratum, the speckles in the transition zone easily dissipate, making it difficult to accurately analyze the displacement and strain of the stratum in this area.

During the test, stratum deformation was measured and the corresponding DIC post-processing was performed for every 5 mm pushover displacement. Due to space limitations, this article focuses on the conditions where stratum displacement and strain underwent sudden changes at pushover displacements of 20 mm and 60 mm, referred to as Condition 1 and Condition 2, as well as the maximum pushover displacement of 100 mm, referred to as Condition 3.

### 4.2 Stratum horizontal displacement

Under the pushover effect, the stratum on the right side of the lining served as the initial load-bearing area, transmitting the load to the lining and the stratum on the left. Horizontal displacements of the stratum in Conditions 1, 2, and 3 were observed using DIC technology, as shown in Fig. 8.

In Condition 1, the surrounding stratum was in an initial state of compaction. In consecutive photographs, the speckle displacement changes were not pronounced. The horizontal displacement contour map exhibited irregular variations.

In Condition 2, the horizontal displacement of the stratum rapidly increased and obvious stratification occurred. The displacement contour showed a tilting trend from right to left, indicating the stratum was entering the overturning stage. The maximum horizontal displacement was approximately 13.3 mm, appearing at the top right corner. Upon further observation, it's evident that layering appeared in the stratum near the right arch shoulder of the lining, that is, local grid cells are experiencing uneven contraction. Compared to the initial grid, the maximum horizontal contraction was 8.7 mm.

In Condition 3, the horizontal displacement of the stratum continued to increase, and the stratification became more pronounced. The uneven contraction

phenomenon of local grid cells intensified, extending to the vicinity of the springing line, with its maximum horizontal contraction being 20.2 mm. At the same time, the lining model also exhibited a significant horizontal displacement (22.6 mm), which was close to the displacement of the surrounding stratum, indicating the stratum was entering the dragging stage (i.e., the stratum and lining were moving together).

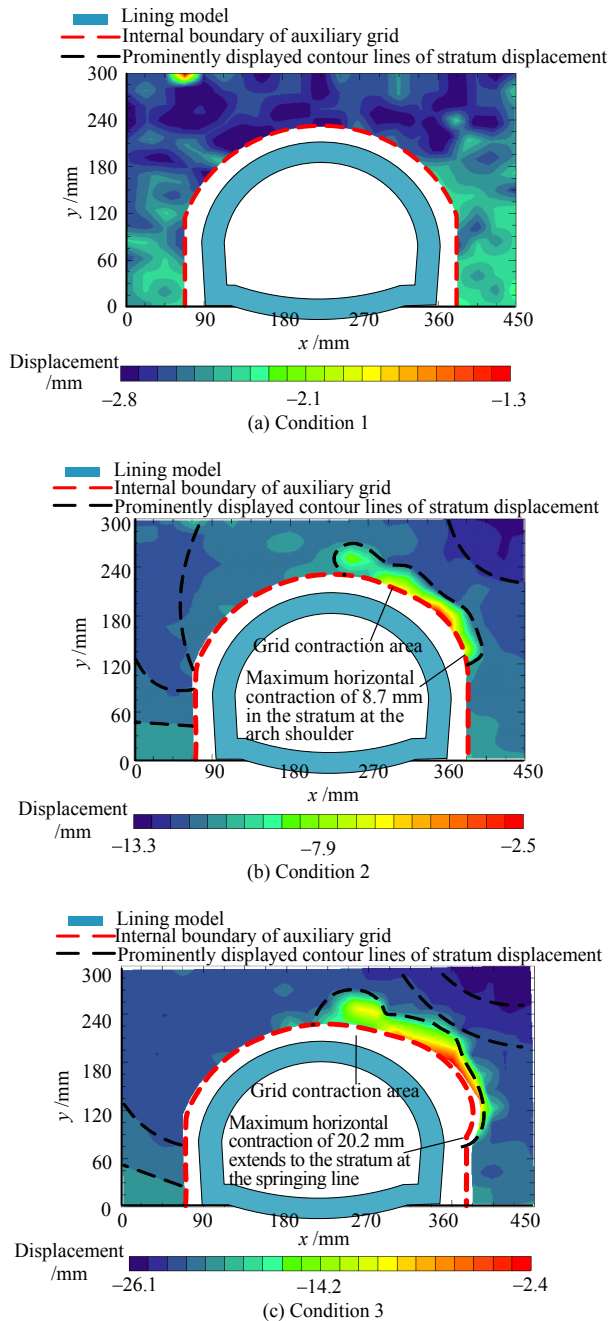


**Fig. 8 Horizontal displacement contour of stratum**

**4.3 Stratum vertical displacement**

Analogously, we focus on the vertical displacements of the stratum in Conditions 1, 2, and 3, as shown in Fig. 9.

In Condition 1, the surrounding stratum was in an initial state of compaction. Under the pushover displacement, the stratum as a whole rose and a clear layering phenomenon appeared. The maximum vertical

displacement approximated 1.2 mm, appearing at the top right corner.

In Condition 2, the vertical displacement of the stratum continued to increase, and the layering became even more pronounced, with a maximum uplift of 3.9 mm. Upon further observation, it's evident that the contour lines of vertical displacement near the right springing line have different directions, indicating that the stratum bifurcated at the springing line and underwent a circumferential flow around the springing line. Meanwhile, the horizontal pushover effect was transmitted circumferentially to the vicinity of the arch shoulder, causing uneven contraction in the local grid cells. Compared to the initial grid, its maximum vertical contraction was 0.5 mm.

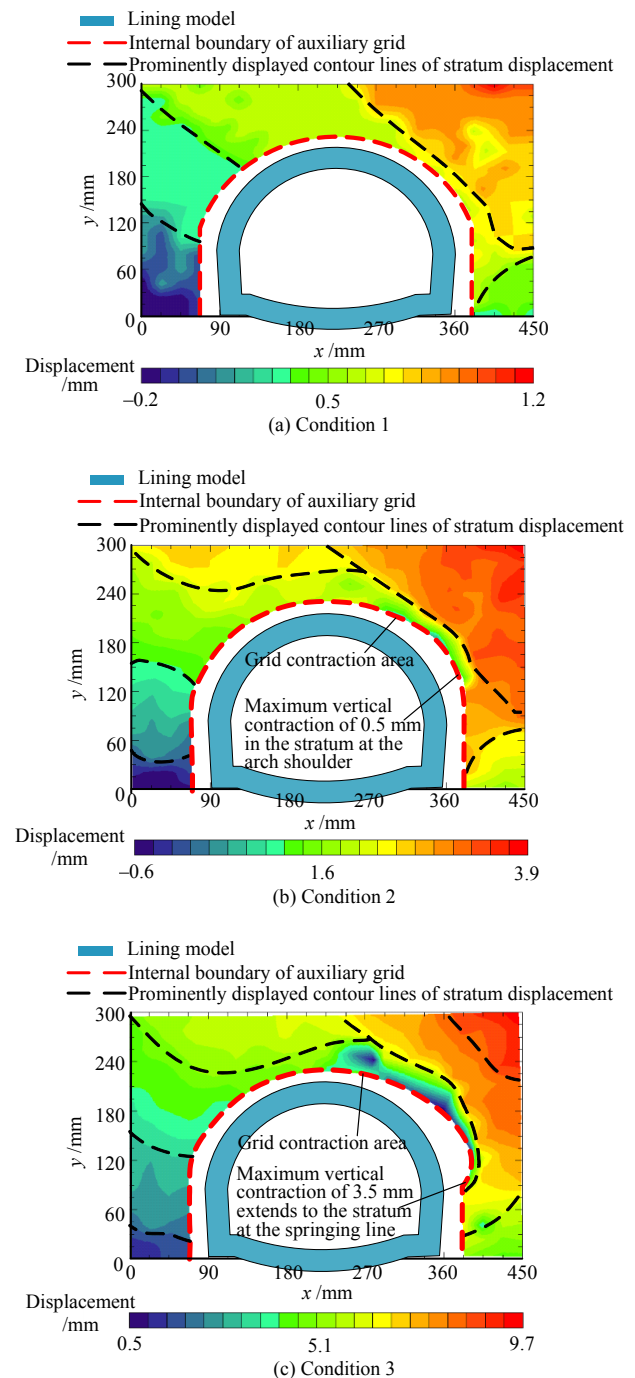


**Fig. 9 Vertical displacement contour of stratum**

In Condition 3, as the pushover displacement increased, the phenomenon of circumferential flow becomes more pronounced. Additionally, the range of grid contraction expanded further to the vicinity of the springing line, with its maximum vertical contraction being 3.5 mm.

## 5 Stratum strain analysis

### 5.1 Stratum compressive strain

Only analyzing the absolute stratum displacement cannot reflect the interaction between the lining and the stratum. Compressive strain is an important indicator reflecting the interaction mechanism between the lining and the stratum. Its contour map is illustrated in Fig.10.

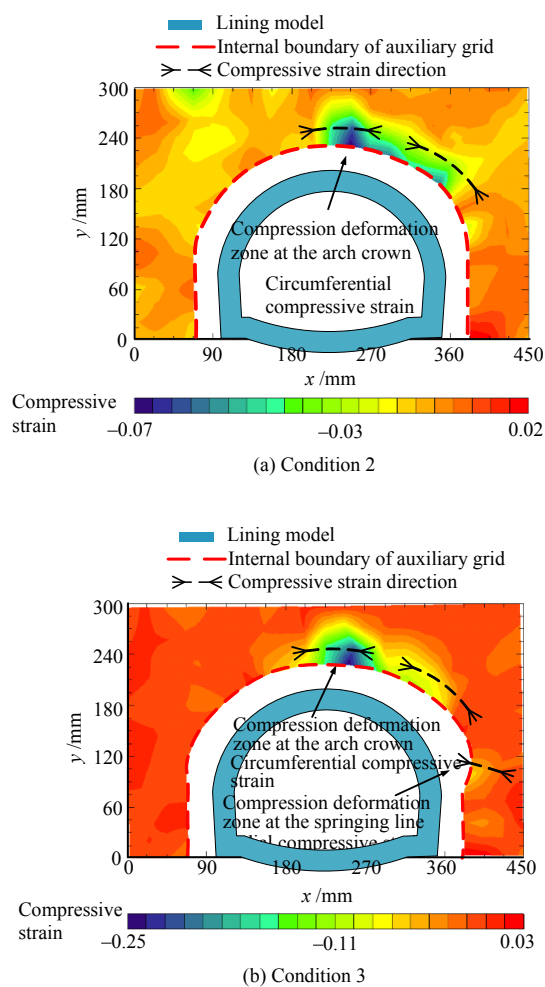


Fig. 10 Stratum compressive strain contour and its direction

In Condition 2, the stratum near the arch crown and the arch shoulder first experienced circumferential compressive strain, forming a compression deformation zone. In Condition 3, with further increase in pushover displacement, the values of circumferential compressive strain in the stratum near the arch crown and arch shoulder significantly increased. At the same time, radial compressive strain appeared in the stratum near the springing line, forming a new compression

deformation zone. The development process of the aforementioned compression deformation zones further corroborates the conclusion that the stratum bifurcates at the springing line and transmits the horizontal pushover effect circumferentially to the vicinity of the arch shoulder/crown.

### 5.2 Stratum tensile strain

Similarly, the contour map of the stratum tensile strain is illustrated in Fig. 11.

In Condition 2, the stratum near the arch shoulder was circumferentially compressed, resulting in radial tensile strain and forming a slip deformation zone. In Condition 3, with the further increase in pushover displacement, the radial tensile strain values in the stratum near the arch shoulder and the arch hance significantly increased. The slip deformation zone expanded to the vicinity of the springing line, and its direction shifted from radial to circumferential. This further corroborated the conclusion regarding the circumferential flow of the stratum.

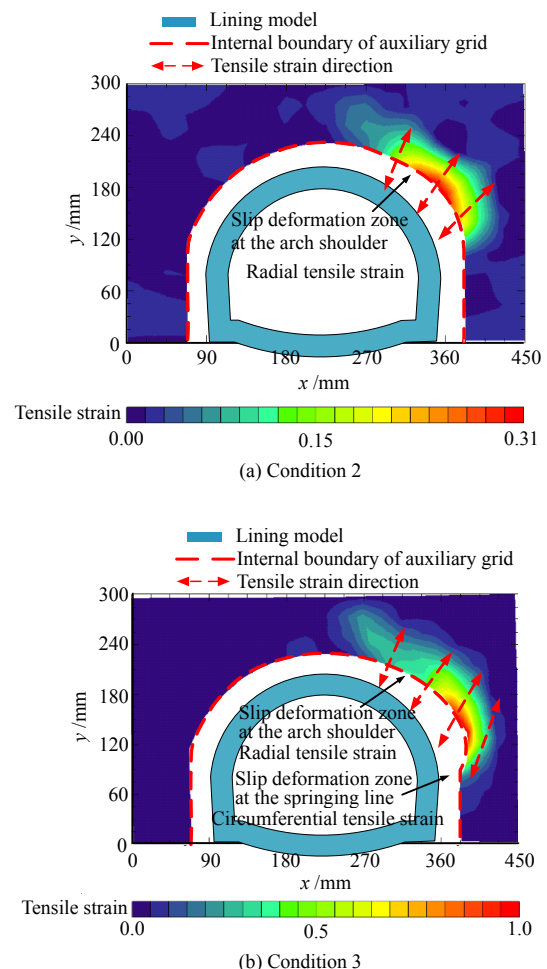


Fig. 11 Stratum tensile strain contour and its direction

## 6 Ground pressure distribution

The ground pressure is a direct manifestation of the interaction between the lining and the stratum. This study focuses on the changes in the ground pressure during the pushover process (i.e., zeroing the

acquisition instrument channel before the test).

### 6.1 Lower ground pressure

The variation of the lower ground pressure (measurement points T6 to T9) with pushover displacement is depicted in Fig. 12. As shown in the figure, the ground pressure at each measurement point generally increased with pushover displacement. Comparing at the same elevation, the ground pressure on the lower right side (represented by the red line) was evidently higher than that on the lower left side (blue line). This is consistent with the findings that the stratum on the lower right side is in a compression deformation zone. Comparing the same lateral position, the sidewall ground pressure was significantly greater than that at the springing line. This was in line with the conclusion that the stratum circumferentially flows around the springing line, and the horizontal pushover effect was transmitted circumferentially.

By further analyzing, the three stages of interaction between the lining and the stratum were identified distinctly from the variation curve of the lower ground pressure. In the initial compaction stage, the stratum and lining mutually compress, causing a rapid rise in ground pressure at each measurement point. After entering the overturning stage, the ground pressure continued to grow steadily. In the dragging stage, the grid contraction zone expanded to the vicinity of the springing line, causing a slight decline in ground pressure there, while the ground pressure at other measurement points once again rose rapidly. When the pushover displacement reached 100 mm, the maximum ground pressure on the right sidewall reached 15.2 kPa.

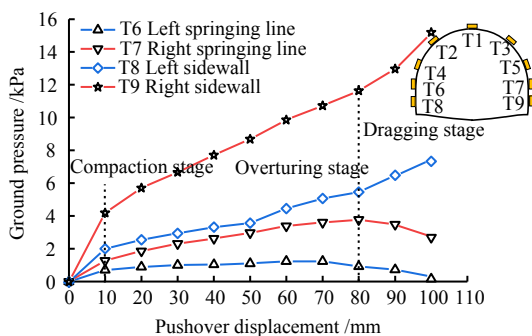


Fig. 12 Variation of lower ground pressure with pushover distance

### 6.2 Upper ground pressure

The variation of upper ground pressure (measurement points T2 to T5) with the pushover displacement is plotted in Fig. 13. It can be observed that the ground pressure at each measurement point generally increased with the pushover displacement. Analyzing from the perspective of stratum strain, it's believed that the upper right stratum was in a sliding deformation zone, characterized mainly by circumferential compression and radial detachment. Therefore, when comparing at

the same elevation, the ground pressure on the upper right (represented by the red line) was clearly less than that on the upper left (blue line). The closer to the arch crown, the more the interaction between the lining and rock was dominated by sliding (rather than by compression). Hence, when comparing at the same lateral position, the ground pressure at the arch hance was significantly higher than that at the arch shoulder.

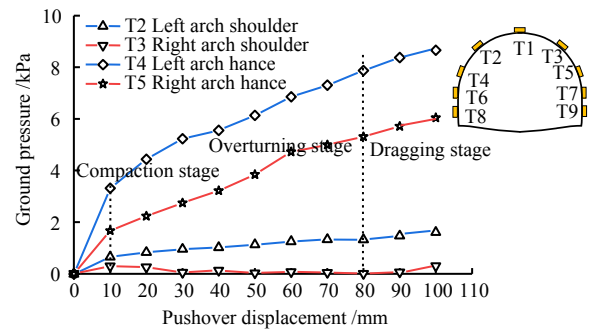


Fig. 13 Variation of upper ground pressure with pushover distance

Similarly, the variation curve of the upper ground pressure also clearly presented three stages of compaction, overturning, and dragging in the interaction between the lining and the stratum, which will not be elaborated further.

## 7 Lining–stratum interaction mechanism

Integrating the aforementioned analyses of stratum displacement, stratum strain, and ground pressure, the interaction mechanism between the tunnel lining and the stratum under static pushover action in the mountain tunnel is illustrated as shown in Fig. 14.

(1) Compaction stage: The stratum begins to compact and undergo regular tilting, which approximates an inverted triangle loading mechanism. Isolines of stratum displacement distribute linearly along the elevation with a certain slope, as shown in Fig. 14(a). In this stage, the ground pressure at each monitoring point increases rapidly.

(2) Overturning stage: As the pushover displacement increases, the circumferential flow of the stratum occurs near the springing line. The isolines of displacement above the arch crown overlie the lining, presenting a large inclination, as depicted in Fig. 14(b). During the overturning process, the slip deformation zone and compression deformation zone form at the arch shoulder and the arch crown, respectively, and the ground pressure at each monitoring point continues to rise steadily.

(3) Dragging stage: As the pushover displacement further increases, the stratum drives the lining to shift together. The isolines of displacement further incline to the left side of the lining, as shown in Fig.14(c).

The slip deformation zone expands to the vicinity of the springing line, causing its ground pressure to slightly decrease, while the ground pressure at other monitoring points continues to increase.

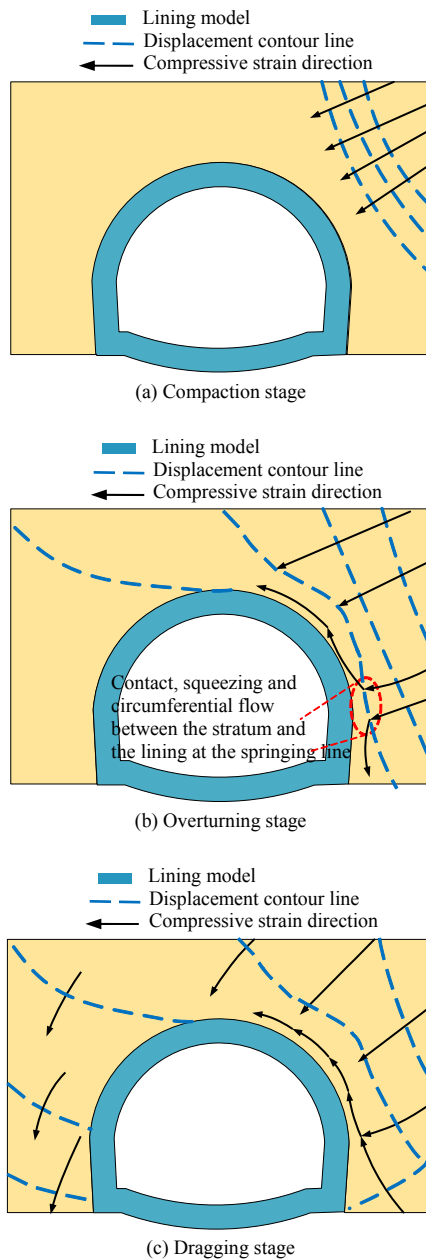


**Fig. 14 Mountain tunnel–stratum interaction mechanism under static pushover action**

Further discussion is made on the failure mode of the lining structure under the extreme condition (further pushing until the lining structure fails). Taking the right springing line as the boundary, the lining in the lower compression zone blocks the stratum displacement, and the lining in the upper slip zone is affected by the stratum flow. This causes the lining at the springing line to first undergo shear failure, forming a through crack ①. After the closed arch structure is broken, cracks ②, ③, and ④ appear in the lining as the squeezing effect further increases, as shown in Fig. 15.

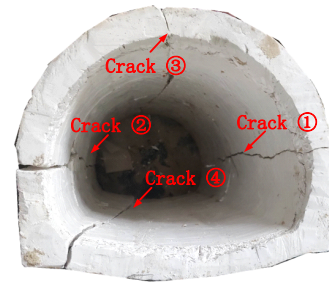


**Fig. 15 Lining cracks under ultimate condition**

## 8 Conclusion

Based on a conventional two-lane highway tunnel section with V-grade surrounding rock as a prototype, a static pushover model test was conducted. The study focused on analyzing the variation rules of stratum displacement, stratum strain, and ground pressure with pushover distance. The interaction mechanism between the mountain tunnel lining and the surrounding stratum was explored. The main conclusions are drawn as follows:

(1) Under horizontal pushover action, the lining–stratum interaction mode can be divided into three stages: compaction, overturning, and dragging. In the overturning stage, the stratum tends to circumferentially flow along the lining perimeter from the springing line. In the dragging stage, the stratum drives the lining to shift together.

(2) In the overturning and dragging stages, the stratum near the arch shoulder mainly undergoes circumferential compression, supplemented by radial expansion, forming a slip deformation zone. Meanwhile, the stratum around the arch crown and the springing line is horizontally squeezed due to the pushover action, forming a compression deformation zone.

(3) The response patterns of the ground pressure on the left and right sides are precisely opposite: In the right-side compression zone, the radial compressive strain causes the pushover effect to be transmitted in the stratum sequentially, resulting in a higher ground pressure than that on the left. In contrast, the compressive strain in the right-side slip zone is circumferential while the tensile strain is radial, causing the stratum to detach from the lining and leading to a lower ground pressure than that on the left.

## References

- [1] PENG Jian-bing, CUI Peng, ZHUANG Jian-qi. Challenges to engineering geology of Sichuan-Tibet railway[J]. Chinese Journal of Rock Mechanics and Engineering, 2020, 39(12): 2377–2389.
- [2] ZHANG X P, JIANG Y J, KAZUHIKO M. Mountain tunnel under earthquake force: a review of possible causes of damages and restoration methods[J]. Journal of Rock Mechanics and Geotechnical Engineering, 2020, 12(2): 414–426.
- [3] WANG T T, KWOK O L, JENG F S. Seismic response of

- tunnels revealed in two decades following the 1999 Chi-Chi earthquake (Mw 7.6) in Taiwan: a review[J]. *Engineering Geology*, 2021(2): 106090.
- [4] JING Li-ping, XU Kun-peng, CHENG Xin-jun, et al. Study on response characteristics of soil-underground structure under horizontal pushover[J]. *Chinese Journal of Geotechnical Engineering*, 2022, 44(9): 1567–1576.
- [5] XU Kun-peng, JING Li-ping, CHENG Xin-jun, et al. Feasibility study of pushover test of underground structure based on boundary displacement method[J]. *Rock and Soil Mechanics*, 2022, 43(1): 127–138.
- [6] CHEN Zhi-yi, LIU Wen-bo, CHEN Wei. Performance experiment of a multistory subway station[J]. *Journal of Tongji University (Natural Science)*, 2020, 48(6): 811–820.
- [7] XU Cheng-shun, HAN Run-bo, DU Xiu-li, et al. Static pushover test technology of spring-underground structure system considering soil-structure interaction and its experimental study[J]. *Journal of Building Structures*, 2023, 44(1): 248–258.
- [8] LIU Jing-bo, AN Zhi-yao, BAO Xin. Study on the influence of soil size in pseudo-static test of soil model box for seismic performance of underground structure[J]. *Earthquake Engineering and Engineering Dynamics*, 2021, 41(3): 11–21.
- [9] HAN Run-bo, XU Cheng-sun, DU Xiu-li, et al. Optimization of model box type in quasi-static pushover test of soil-underground structure system[J]. *Rock and Soil Mechanics*, 2021, 42(2): 462–470.
- [10] WANG X, PAN C. Review of seismic damage characteristics and influence factors of mountain tunnels[J]. *Arabian Journal of Geosciences*, 2022, 15(6): 1–16.
- [11] GUAN Zhen-chang, GONG Zhen-feng, LUO Zhi-bin, et al. Seismic property of a large section tunnel based on shaking table model tests[J]. *Rock and Soil Mechanics*, 2016, 37(9): 2553–2560.
- [12] Ministry of Housing and Urban-Rural Development of the People’s Republic of China. GB 50909—2014 Code for seismic design of urban rail transit structures[S]. Beijing: Standards Press of China, 2014.
- [13] Ministry of Transport of the People’s Republic of China. JTG/T 2232-01—2019 Specification for seismic design of highway tunnels[S]. Beijing: China Communications Press, 2019.
- [14] LIU Jing-bo, WANG Wen-hui, ZHAO Dong-dong, et al. Integral response deformation method for seismic analysis of underground structure[J]. *Chinese Journal of Rock Mechanics and Engineering*, 2013, 32(8): 1618–1624.
- [15] HAN Run-bo, XU Cheng-sun, XU Zi-gang, et al. A boundary forced response displacement method for seismic analysis of symmetrical underground structures[J]. *Engineering Mechanics*, 2021, 38(5): 50–60.
- [16] GUAN Zhen-chang, LUO Zhi-bin, XU Qiu, et al. Seismic responses of large section tunnel based on shaking table model test[J]. *Journal of Engineering Geology*, 2017, 25(3): 648–656.
- [17] WANG Shu-ping. Model test study on tunnel within cracked surrounding rock[D]. Hangzhou: Zhejiang University, 2004.
- [18] LI Yuan-hai, LIU De-zhu, YANG Shuo, et al. Experimental investigation on surrounding rock stress and deformation rule of TBM tunneling in deep mixed strata[J]. *Rock and Soil Mechanics*, 2021, 42(7): 1783–1793.